Wireless Communication Based on Chirp Signals for LoRa IoT Devices

Article · December 2018

CITATIONS
6

READS
6,774

2 authors:

Vitor Manuel Fialho
Instituto Politécnico de Lisboa
19 PUBLICATIONS **24** CITATIONS
SEE PROFILE

Fernando Azevedo
Instituto Politécnico de Lisboa
36 PUBLICATIONS **39** CITATIONS
SEE PROFILE

i-ETC: ISEL Academic Journal of Electronics, Telecommunications and Computers
IoT-2018 Issue, Vol. 4, n. 1 (2018) ID-6

Wireless Communication Based on Chirp Signals for LoRa IoT Devices

V. Fialho[ab], F. Azevedo[a]
[a]Área Departamental de Engenharia Electrónica e Telecomunicações e de Computadores - ADEETC, ISEL, Portugal
[b] Centre of Technology and Systems – CTS, UNINOVA, FCT, Portugal
vfialho@deetc.isel.ipl.pt fazevedo@deetc.isel.ipl.pt

Abstract **— This paper presents the study of chirp signals for wireless communications between Internet of Thing devices used on low power wide area networks. Up and down chirp concept is introduced as well as the chirp spread spectrum concept. A computationally efficient symbol decoding method is presented based of discrete Fourier transform as an alternative to typical coherent detection. The proposed LoRa simulation model is implemented in MATLAB allowing the communication system evaluation based on bit error rate and packet error rate.**

Keywords: Chirp signal, spread-spectrum, IoT, spreading factor, bit error rate packet error rate, signal to noise ratio.

I. INTRODUCTION

Internet of Things (IoT) concept emerged several years ago supporting the actual topic of smart cities. Actually, every object (thing) can be monitored by transmitting information about a specific context and environment. The main paradigm of IoT is the ability to connect to Internet with a low cost, limited infrastructure and a very long life time battery, e.g. low power wide area network LPWAN [1].

Several standards support wireless communication between IoT devices and each device to Internet, using gateways [1]. Each standard has different specifications, however they can be divided in two major categories: short range (less than 100 meters radius) and long range (greater than 1000 meters radius). First category includes protocols such as IEEE 802.15.4, ZigBee and Bluetooth. Second category includes system architecture and protocols similar to cellular network [1][2][3].

From the several LPWAN standards presented in [2][3], SigFox® [4] and LoRa (Long Range modulation), defined by LoRa® Alliance [5], are spreading faster than others LPWAN [6]. Both protocols operate across instrumental, scientific and medical frequency bands (ISM).

SigFox® standard allows a limited uplink and downlink messages per day. In order to access the information, a subscription fee is paid [4][6].

LoRa® is an open protocol, defined by the nonprofit association LoRa® Alliance [5]. This protocol allows the creation of a private network with no data traffic limitation, packet size and no subscription fee need to be paid [6]. The frequency band allocated for European Union is 868 MHz with configurable bandwidth. One last feature of LoRa® protocol is the duty-cycle, which may assume values between 0,1% to 1% of total transmitting time [5].

Figure 1 presents a simplified LoRa® architecture in which are represented the end-device managed by a micro-controller, LoRa® gateway, data base and a personal computer to access the stored data.

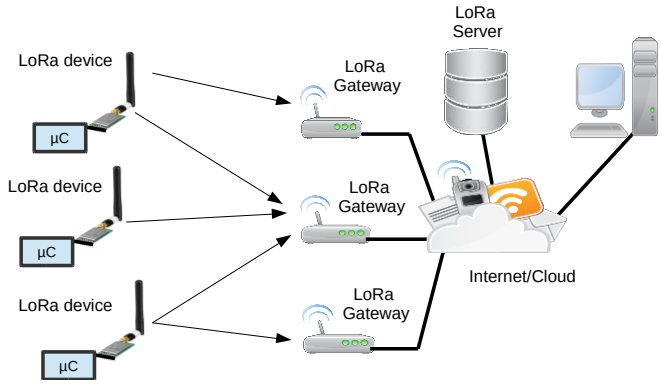

Fig. 1. LoRa simplified network concept.

This paper presents the study of LoRa® wireless radio communication between the end device and the gateway. The modulation is based on chirp signals. Therefore, the chirp spreading spectrum modulation concept is presented, such as a computationally efficient method for demodulation and decoding chirp signals. This method is based on discrete Fourier transform (DFT). A simulation model developed in MATLAB is presented, allowing the performance assessment in presence of additive white Gaussian noise (AWGN). The obtained simulation results are based on bit error rate (BER) and packet error rate (PER).

II. LORA CHIRP SPREADING SPECTRUM MODULATION

LoRa® wireless communication is based on chirp spread-spectrum (CSS) modulation scheme [5][6][7][8][9]. Chirp signal with in-phase (I) and quadrature (Q) is given by (1),

$$s(t) = e^{j(2\pi f_c t + 2\pi \frac{\beta}{2} t^2)} \quad (1)$$

where f_c is frequency carrier, β is frequency variation slope given by the ratio between bandwidth (BW) and time symbol (T_{symb}), as expressed by (2) [7][9]

$$\beta = \frac{BW}{T_{symb}}, \quad (2)$$

time symbol is given by (3)

$$T_{symb} = \frac{2^{SF}}{BW} . CR, \quad (3)$$

where SF is the spreading factor, e.g., number of bits per encoded symbol, and CR the code rate [7].

Figure 2 presents two signals normalized to T_{symb}: up-chirp (β>0) and a down-chirp (β<0). Assuming $BW=f_1-f_0$ with $f_1 > f_0$ positive slope is obtained, otherwise slope is negative.

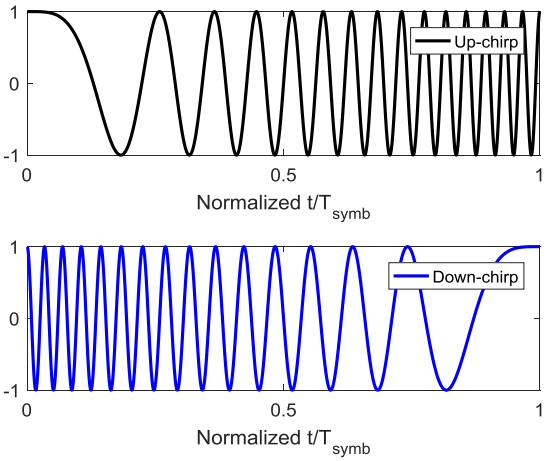

Fig. 2. Up and down chirp signals normalized to T_{symb}.

Chirp frequency variation can be represented as depicted in Figure 3. This graphical analysis allows T_{symb} estimation within a specific *BW*. It is also possible to infer the chirp slope.

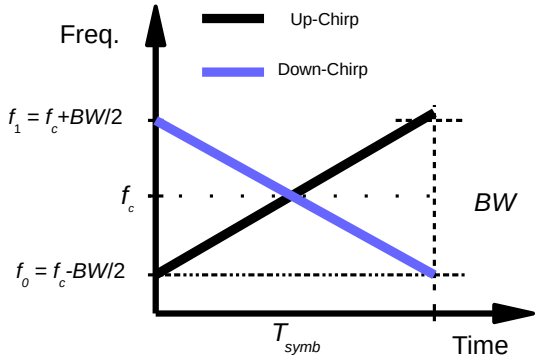

Fig. 3. Spectrogram representation: up-chirp and down-chirp.

According to LoRa® specification the *BW*, *SF* and *CR* may assume the values presented on Table I [7].

TABLE I
LORA® MODULATION MAIN PARAMETERS

Bandwidth (BW)	125 kHz to 500 kHz
Spreading Factor (SF)	7 to 12
Coding Rate (CR)	1 to 4

LoRa packet, presented in Figure 4, contains a preamble, composed by six up-chirps and two down-chirps configured with a specific SF and BW values. Data field contains optional header payload and payload cyclic redundancy check (CRC) value [6]. The CR value in this filed may change between the values presented in Table I.

Fig. 4. LoRa packet composed by preamble and data fields.

A. CSS Symbol Coding and Modulation

LoRa® CSS technique allows symbol generation depending on the SF value, for a specific bandwidth. If only chirp slope variation were used to encode digital data, only two different symbols were generated. In CSS symbol coding and modulation is based on *SF* value within a fixed *BW*.

As analogy to digital modulation, *SF* corresponds to the number of bits per symbol. Therefore, according to (3), with *SF*=7 it is possible to encode 128 symbol during a T_{symb} within a given *BW*. In order to distinguish each symbol, using a chirp signal, a cyclic shift (*cs*) is used according to (4)

$$cs = \frac{sv}{2^{SF}} T_{symbol} \ , \tag{4}$$

where *sv* corresponds to the symbol value (0 to 2^{SF}-1), and the reference symbol is an up-chirp with *sv*=0. This shift encoding increases the number of symbols in a factor of 2^{SF}. For *sv*=16, the deviation from reference chirp is 16/128 of T_{symbol}.

Figure 5 show the spectrogram estimation for two *sv* values: 16 and 112 for a SF=7.

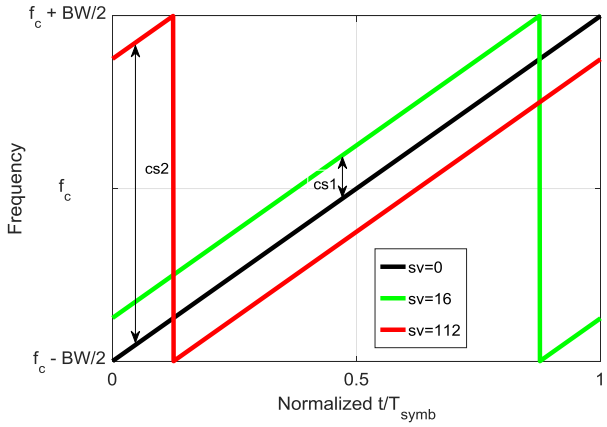

Fig. 5. Chirp cyclic shift for two different symbol with SF=7.

As conclusion, *cs* correspond to a time delay referenced to T_{symbol}. This characteristic enables the demodulation and decoding of 2^{SF} symbols with a computationally efficient method [8].

B. LoRa® Symbol Demodulation and Decoding

LoRa® CSS demodulation process is based on a typical coherent demodulation concept, however the reference signal used for decoding is a down-chirp signal with the same SF used in the modulation process [8][9].

Considering CSS a digital modulation and assuming perfect time and frequency synchronization, as well as symbol source generator with uniform distribution, the optimum receiver can be mathematically described as presented in [8].

For a computationally efficient implementation (discrete signals), the method proposed by [8] consists on the product of the received signal with a down-chirp, corresponding to the complex conjugate of a chirp with *cs*=0.

Figure 6 presents signal operation the block diagram of the proposed method, where d[n] is given by

$$d[n] = r[n] \ . \ s^*[n], \tag{4}$$

where * denotes s[n] complex conjugate, e.g. a down-chirp with *sv*=0.

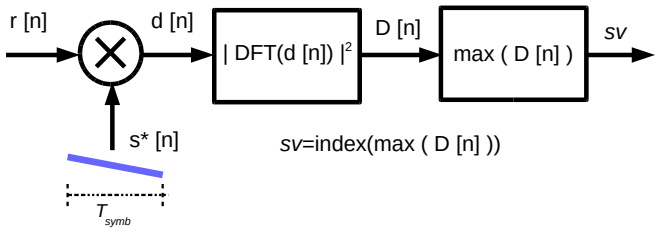

Fig. 6. LoRa® CSS demodulation concept.

D[n] is the DFT square modulus of the signal d[n]. Symbol value, *sv*, corresponds to the index of the maximum value of D[n].

As result of operation described in Figure 6 applied to the chirp signals generated by the *cs* presented in Figure 5, the results are shown in Figure 7.

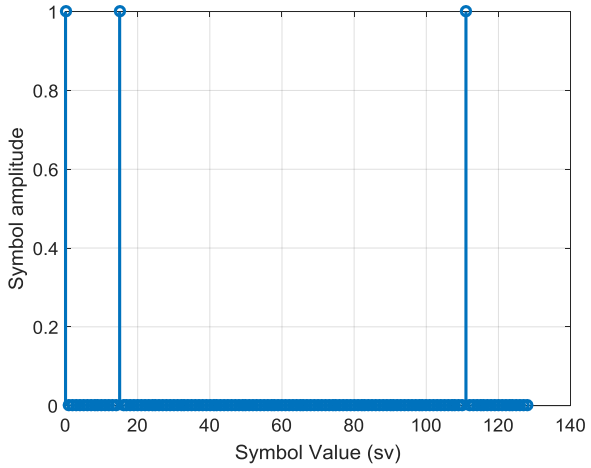

Fig. 7. Decoded LoRa® symbols: 0, 16 and 112.

Since SF is 7, r[n] is composed by 128 samples (0 to 127). Therefore the cyclic shift, *cs*, imposed by coding process will impose the correct symbol decoding.

III. LORA® WIRELESS SIMULATION SCENARIO

In this section it is presented the simulation system developed in MATLAB which implements CSS modulation described in section II. The simulator block diagram is presented in Figure 8.

Symbol mapping is generated according to Gray code which ensures that adjacent symbols are mapped to bit patterns differing in one position only [9].

The output chirp signal, CS, depends on spreading factor (*SF*), frequency carrier (f_c) and bandwidth (*BW*). The channel model is based on AWGN with a configurable SNR.

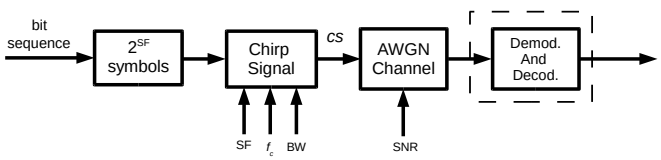

Fig. 8. LoRa® CSS MATLAB simulation model.

Surrounded block with the dashed line, composed by the demodulator and decoder, is implemented with the algorithm proposed in section II-B and represented in Figure 6.

As mentioned in section I, in EU, LoRa® frequency band is allocated in 868 MHz, however the frequency carrier used for the simulations where smaller in order to ensure that simulation time would be feasible. Therefore all the results are normalized to f_c.

A. Simulation Results – Spreading Factor

The spectrogram of three up-chirps with 125 kHz bandwidth is presented in Figure 9 for a SNR=10 dB. The *SF* values used for each chirp signal are 7, 8 and 9 with *CR* = 1. These configurations lead to a T_{symb} of 1ms, 2ms and 4ms.

In conclusion, increasing *SF* a factor by one, the time symbol duration doubles, according to expression (3).

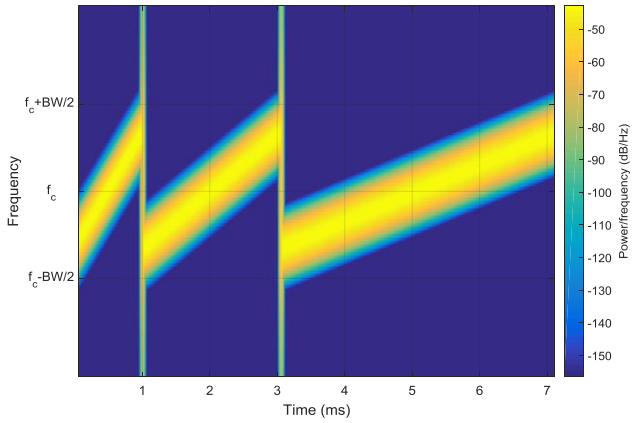

Fig. 9. LoRa® CSS symbols with SF 7,8 and 9.

B. Simulation Results – Symbol Demodulation and Decoding

Figure 10 presents LoRa® CSS spectrogram preamble with *SF*=7, composed by six up-chirps and two down chirps [7] followed by symbols 0, 16 and 112.

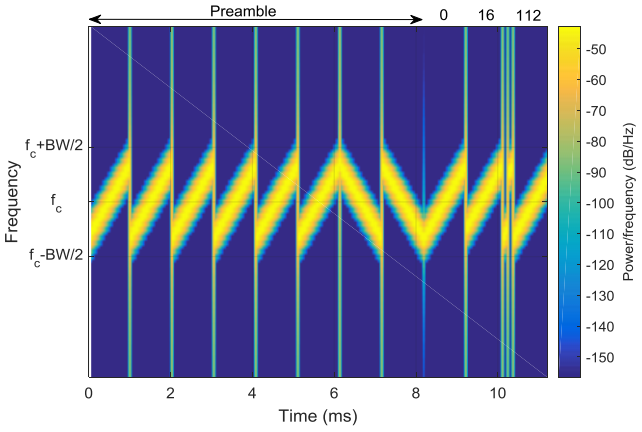

Fig. 10. LoRa® CSS packet spectrogram with SF = 7 with symbols 0, 16 and 112.

For each received CSS symbol, r[n], the demodulation and decoding process presented in Figure 6 is performed. After discarding the preamble, D[n] signals for symbols 0, 16 and 112 are presented in Figure 11. As it turns out, index of D[n] maximum value corresponds to the transmitted *sv*.

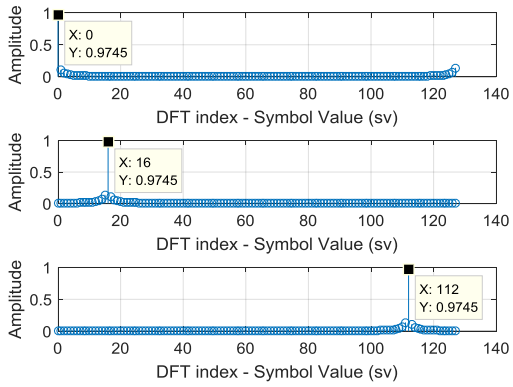

Fig. 11. CSS DFT D[n] signals for symbols 0, 16 and 112.

Figure 12 presents LoRa packet for SNR=-10 dB. As depicted, CSS power spectral density is less defined due to AWNG noise influence. Nevertheless up and down chirps can be identified. The noise impact on CSS modulation is described in next section.

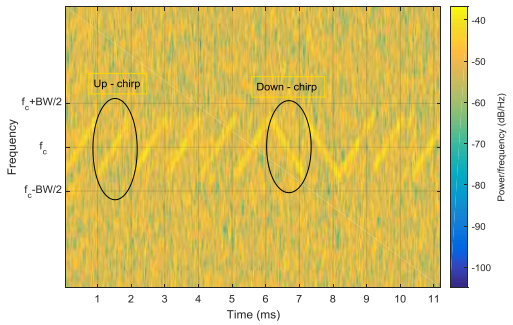

Fig. 12. . LoRa® CSS packet spectrogram with SF = 7 for SNR = -10dB.

IV. LoRa Model Evaluation: BER and PER

To infer system evaluation under noise condition, MATLAB simulation scenario generates 20000 symbols based on binary sequence with a uniform distribution, grouped in 2^{SF} values with Gray coding.

Figure 13 show first fifty coded and decoded symbols for SNR=-10 dB with a *SF*=7. The obtained results denote the errors between the coded and decoded symbols.

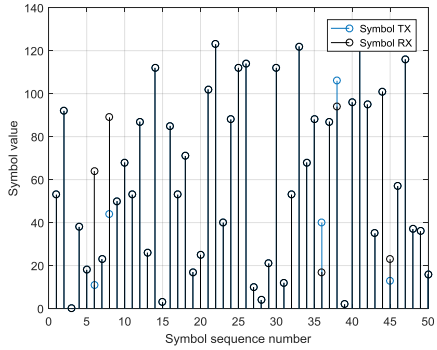

Fig. 13. First 50 LoRA® CSS decoded symbols (SF=7) with SNR=-10 dB.

AWGN impact on LoRa® CSS modulation is evaluated based on BER. This evaluation is preformed comparing the MATLAB binary sequence and the decoded one. The obtained results are compared with work [8], under the same noise conditions, as presented in Figure 14.

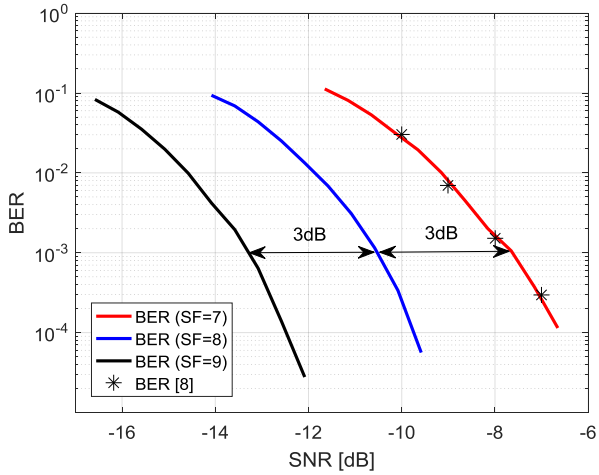

Fig. 14. Simulation results based on BER for SF 7, 8, 9 and work [8].

Assuming system reference BER=10^{-3}, for each *SF* increase, the SNR decrease 3dB. Therefore, if channel noise conditions decreases, to achieve the same performance, the *SF* needs to increase. Assuming CSS link budget project, to achieved greater distances, *SF* value must increase [7], however symbol rate decreases.

Another LoRa® CSS modulation evaluation performance is based on PER values. This is a useful parameter, since several LoRa® modules allow PER measurement such as SX1276 [10].

LoRa® packet preamble is used for synchronization, therefore if one of the six decoded symbols is incorrect, the packet is discarded, and an error is incremented.

For PER simulation 10000 packets where generated and each preamble analyzed. The obtained values are presented in Table II.

TABLE II
PER SIMULATION RESULTS FOR DIFFERENT SF VALUES

	PER	
SF	SNR=-13 dB	SNR=-11 dB
7	38,7%	19,1%
8	9,5%	0,8%
9	0,02%	n.a

Based on the obtained values it is possible to infer that PER is approximately similar to BER, under the same CSS modulation parameters and noise channel conditions.

V. Conclusions

A chirp spreading spectrum modulation scheme for LoRa® wireless communication has been presented, based on computationally efficient decoding method (DFT).

A simulation model is presented which enables the chirp signal configuration as well as channel noise conditions, which allows system performance assessment based on BER and PER. The obtained results show that CSS modulation configuration parameters results on a trade of on binary rate, channel noise conditions and, consequently, the link budget between LoRa module and the gateway.

The main advantage of CSS modulation comparing with other binary modulations is the occupied bandwidth, computationally efficient symbol decoding and power consumption.

For future work we propose to improve the simulation model in order to evaluate signal interference between modules. Therefore we need to adapt the proposed model to LoRa® channel access and, under these conditions, evaluate BER and PER. For experimental validation it will be used SX1276 modules [10].

REFERENCES

[1] K. Nolan, et al. An Evaluation Of Low Power Wide Area Network Technologies For The Internet Of Things, in Proc. of IWCMC 2016–IEEE International Wireless Communications and Mobile Computing Conference, Paphos, Cyprus, Sep. 2016, pages 439-444.

[2] S. Al-Sarawi, et al. Internet of Things (IoT) communication protocols: Review, in Proc. of ICIT 2017–IEEE 8th International Conference on Information Technology, Amman, Jordan, May. 2017, pages 685-690.

[3] O. Khutsoane, et al. IoT Devices and Applications based on LoRa/LoRaWAN, in Proc. of IECON 2017–43rd Annual Conference of the IEEE Industrial Electronics Society, Beijing, China, Nov. 2017, pages 6107-6112.

[4] SigFox, "About SIGFOX." [Online]. Available: http://www.sigfox.com/en/#!/about.

[5] "LoRa Technology." [Online]. Available: https://www.lora-alliance.org/.

[6] L. Angrisani, et al. LoRa Protocol Performance Assessment in Critical Noise Conditions, in Proc. of RTSI 2017–IEEE 3rd International Forum on Research and Technologies for Society and Industry, Modena, Italy, Sep. 2017.

[7] LoRa™ Modulation Basics, AN1200.22 Application Note-[Online]Available: https://www.semtech.com/uploads/documents/an1200.22.pdf..

[8] L. Vangelista, et al. Frequency Shift Chirp Modulation: The LoRa Modulation, in IEEE Signal Processing Letters, vol.24, no. 12, pages 1818-1821, Dec. 2017.

[9] D. Croce, et al. Impact of LoRa Imperfect Orthogonality: Analysis of Link-Level Performance, in IEEE Communications Letters, vol. 22, no. 4, pages 796-799, Apr. 2018.

[10] SEMTECH WIRELESS, SENSING & TIMING, SX127X Datasheet, [Online] Available: https://www.semtech.com/uploads/documents/DS_SX1276-7-8-9_W_APP_V5.pdf.